

EFFECTS OF OPERATING AND GEOMETRIC PARAMETERS ON CaSO_4 CRYSTALLIZATION FOULING IN PLATE HEAT EXCHANGERS

K.S. SONG¹, S.W. KIM¹, H. KANG², C.H. BAEK² and Y. KIM^{2*}

¹Graduate School of Mechanical Engineering, Korea University, Seoul 136-713, Korea

²Department of Mechanical Engineering, Korea University, Seoul 136-713, Korea

*E-mail: yongckim@korea.ac.kr

ABSTRACT

Plate heat exchangers have been widely used in a district heating system. The fouling is unwanted deposit on the heat exchanger surface. Crystallization fouling is major mechanism to cause many problems for industrial applications. The objective of this study is to investigate the effects of calcium sulfate (CaSO_4) crystallization fouling on the performance of the plate heat exchangers under various operating and geometry conditions such as concentration, inlet temperature, flow velocity, and chevron angle. The tests were conducted under accelerated concentration conditions. The fouling resistance showed an asymptotically increasing curve. The fouling resistance increased with the increase in the chevron angle, concentration, and inlet temperature, whereas decreased with the increase in the flow velocity. In addition, the overall heat transfer coefficient decreased and pressure drop increased with the increase in the fouling resistance.

INTRODUCTION

Recently, many studies on the improvement of energy efficiency throughout a wide range of industrial fields have been conducted because the development of environment friendly technologies and the depletion of fossil energy are becoming main issues. The research and development of a highly efficient heat exchanger have been required for the efficient management of energy and the recovery of waste energy. Therefore, the selection of appropriate high-efficiency heat exchanger affects the efficiency of the manufacturing process and reduction of the total energy management cost. Plate heat exchangers (PHEs) began to be used in various industrial fields due to small area of installation, ease of maintenance and high heat transfer efficiency compared to shell and tube heat exchangers.

In the water heating system such as district heating and hot water service, the crystallization fouling often causes performance degradation in PHEs because insoluble salts are precipitated on the surface in the supersaturated aqueous solution. Generally, the solubility of a normal salt increases with an increase in the temperature. However, some salts show inverse solubility, such as calcium carbonate (CaCO_3) and sulfate (CaSO_4). The solubility of CaSO_4 decreases with the increase in the water temperature after 40°C consistently.

Since the discharge temperature of usable water is up to the high temperature above 40 °C in the district heating and service hot water systems with a cooling tower, the crystallization fouling effect on the thermal performance is especially very important in these fields.

Fouling in heat exchangers has been studied in various fields. Genić et al. studied the relationship the flow rate and the fouling resistance, and the experiments were conducted in the heating condition for one year without accelerated concentration that means the concentration is a hundred times higher than normal water one to decrease scale formation times. However, because of long measurement time, recently fouling research is being conducted under accelerated concentration condition. Bipan Bansal et al. studied the deposition of calcium sulphate in two different plate heat exchanger geometries. T.M Paakkonen et al. studied surface crystallization and crystallization in the bulk fluid and its effect on the mass deposition on a heated surface. Moriz Mayer et al. studied the impact of crystallization fouling on the heat transfer performance of a micro heat exchanger. Thonon et al. studied that the fouling resistance curve increased asymptotically with time and was inversely proportional to the flow rate from the experiment under accelerated concentration condition. However, previous researches were conducted under low temperature conditions for an open cycle system. Therefore, their studies were different from the phenomenon in the actual heating system.

Even with such extensive studies on the crystallization fouling in PHEs, the data on the crystallization fouling characteristics of CaSO_4 under district heating conditions according to operating and geometric parameters have been limited. In this study, the fouling resistance and pressure drop characteristics of PHEs were measured and analyzed under accelerated CaSO_4 crystallization fouling conditions by varying operating and geometrical parameters such as CaSO_4 concentration, inlet temperature, flow velocity, and chevron angle of the heat transfer plate.

EXPERIMENTAL SETUP

Fig. 1 shows the experimental setup used in this study on the effect of CaSO_4 crystallization fouling in PHEs. The

test apparatus consisted of a heating, a cooling unit and a

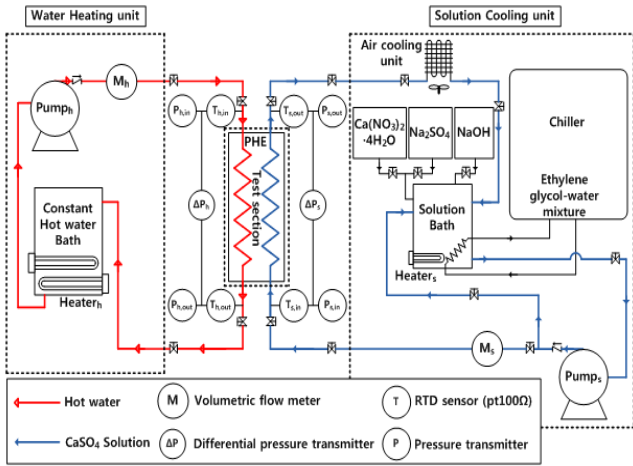


Fig. 1 Schematic diagram of the experimental setup.

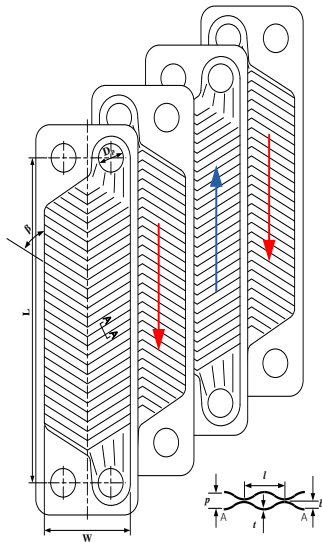


Fig. 2 Schematic diagram of the tested plate.

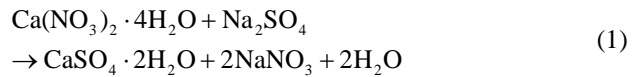
Table 1. Geometrical parameters of the plate.

Geometrical parameters	Value
Plate length	0.357 m
Plate width	0.103 m
Plate thickness	0.0006 m
Plate pitch	0.005 m
Corrugation depth	0.0025 m
Corrugation length	0.01 m
Plate surface area	0.0813 m ²

test section. The heating unit consisted of a hot water bath, heater and an inverter pump. The water entering the test section was heated by heaters with a capacity of 45 kW in the hot water bath with a maximum volume of 500 l. The hot water flow rate was controlled by the inverter pump. The cooling unit consisted of a cooling water bath, heater, chiller, an inverter pump, and air cooling unit. CaSO₄ solution was made in the cooling water bath with a maximum volume of 500 l. After passing through the test section, the heated solution was cooled using the air cooling unit and the water

chiller with the capacity of 17.5 kW and 30 kW, respectively. The test section consisted of a plate heat exchanger with four plates. Fig. 2 shows a schematic diagram of the tested plate. The chevron type plates contained three channels with two outer channels for the hot water and an inner channel for the CaSO₄ solution. The heat was exchanged between the hot water and CaSO₄ solution in a counter flow; the downward flow of the hot water and the upward flow of the solution.

The CaSO₄ reagent cannot be dissolved well at the room temperature because the solubility of CaSO₄ is significantly low at the room temperature and the ionic bonding force of CaSO₄ is higher than that of water molecules. In addition, the undissolved CaSO₄ particles in the solution can affect the crystallization fouling. Therefore, the concentration of the CaSO₄ solution was controlled by mixing calcium nitrate (Ca(NO₃)₂·2H₂O) and sodium sulfate (Na₂SO₄). As given in Eq. (1), Ca(NO₃)₂·2H₂O and Na₂SO₄ were reacted to make a calcium sulfate (CaSO₄). The solution was mixed through the inner circulation pump and the concentration of the solution was checked through concentration measuring instrument to confirm that it was sufficiently mixed.



When the volumetric water flow rate and water temperature reached steady state with respective fluctuations within ±0.01 m³ h⁻¹ and ±0.5 °C compared with the setting conditions, the reagents for CaSO₄ fouling were injected into the solution bath. After controlling the concentration of CaSO₄ solution, the crystallization fouling tests were started. The data were recorded in 1-s intervals. When the temperature and the pressure variation of the solution were within ±0.1 °C and ±10 kPa for one hour, it was defined that the crystallization fouling reached equilibrium state. In the CaSO₄ crystallization fouling test, the CaSO₄ concentrations were varied from 0.4 to 0.6 wt. %. Re was varied from 2500 to 5600 and the flow velocities was varied from 0.33 m/s to 0.76 m/s. The inlet temperature of the solution and the hot water was fixed at 40 and 95 °C, respectively. The chevron angle of the PHE was varied from 30° to 60°.

DATA EVALUATION

The heat transfer rates of the hot water and the solution were calculated using Eq. (2) and (3), respectively.

$$Q_h = \dot{m}_h c_{p,h} (T_{h,in} - T_{h,out}) \quad (2)$$

$$Q_s = \dot{m}_s c_{p,s} (T_{s,out} - T_{s,in}) \quad (3)$$

The energy balance between the hot water-side and the solution-side heat transfer rates was within ±5%. As given in Eq. (4), the average heat transfer rate for the hot water-side and the solution-side was used to calculate the overall heat transfer coefficient.

$$Q_{avg} = (Q_h + Q_s) / 2 \quad (4)$$

The overall heat transfer coefficient was determined in terms of the average heat transfer coefficient, heat transfer area, and logarithmic mean temperature difference.

$$U = Q_{avg} / A \Delta T_{lm} \quad (5)$$

The logarithmic mean temperature difference was expressed by

$$\Delta T_{lm} = \frac{(T_{h,in} - T_{s,out}) - (T_{h,out} - T_{s,in})}{\ln \left[\frac{(T_{h,in} - T_{s,out})}{(T_{h,out} - T_{s,in})} \right]} \quad (6)$$

The heat transfer area A was calculated by applying the enlargement factor (Φ) proposed by Martin. As the CaSO_4 crystallization fouling progressed with time, the overall heat transfer coefficient decreased and the fouling resistance increased. The initial value of the overall heat transfer coefficient at clean state was defined by U_0 . The overall heat transfer coefficient at a given time was defined by U_t . The fouling resistance ($R_{f,t}$) was calculated by the thermal resistance difference between the certain and the initial time. In addition, the thermal performance degradation (U_R) was defined as the ratio of the overall heat transfer coefficient at the certain time to that at the initial time.

$$R_{f,t} = 1/U_t - 1/U_0 \quad (7)$$

$$U_R = U_t / U_0 \quad (8)$$

The pressure drop ratio (ΔP_R) was defined by a function of the initial value of the pressure drop at clean state (ΔP_0) and the pressure drop at a given time (ΔP_t).

$$\Delta P_R = \Delta P_t / \Delta P_0 \quad (9)$$

RESULTS & DISCUSSION

Fig. 3 shows the variation of the thermal performance degradation ratio and the fouling resistance with time at various chevron angles. The CaSO_4 concentration and Re were maintained at 0.6 wt. % and 2512 – 2602, respectively. The inlet temperatures of the hot water and solution were fixed at 95 °C and 40 °C, respectively. In the CaSO_4 crystallization fouling in PHEs, the fouling resistance increased with time and then approached a steady value after a certain period. The asymptotic fouling period decreased with the increase in the chevron angle because the increased deposition rate at the early stage led to higher removal rate simultaneously with the decreased surface temperature.

Fig. 4 shows the variation of the fouling resistance with time at various CaSO_4 concentrations. The Re , chevron angle, and inlet temperatures of the solution and hot water were maintained at 2552 – 2601, 60°, 40 °C, and 95 °C, respectively. Before the asymptotic fouling period, the increasing slope of the fouling resistance increased with the increase in the CaSO_4 concentration because the increased reaction rate with the increased number of foulant ions led to higher deposition rate. The asymptotic fouling resistance increased with the increase in the CaSO_4 concentration

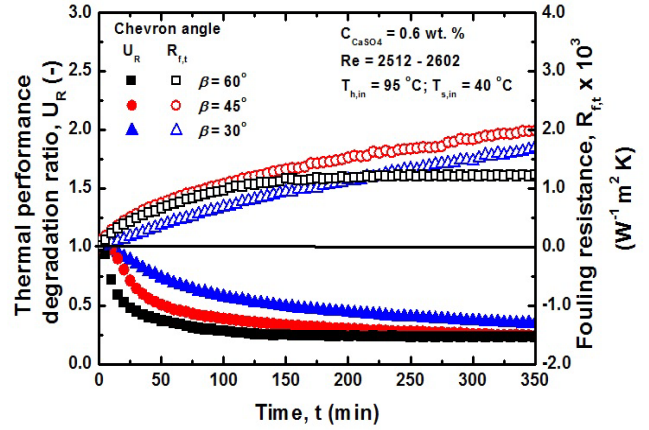


Fig. 3 Effect of chevron angle on the fouling resistance.

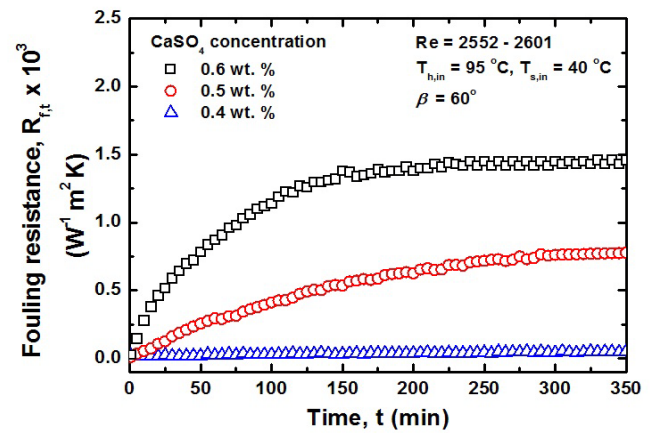


Fig. 4 Effect of CaSO_4 concentration on the fouling resistance.

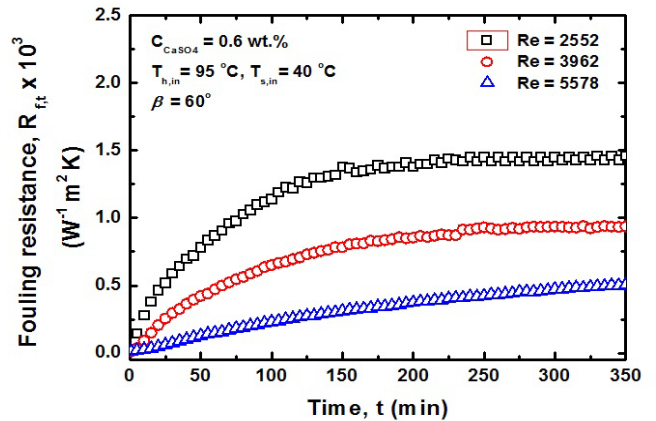


Fig. 5 Effect of Re on the fouling resistance.

because of the increased number of foulant ions. However, the asymptotic fouling period decreased with the increase in the CaSO_4 concentration because the increased deposition rate at the early stage led to higher removal rate with the decreased surface temperature.

Fig. 5 shows the variation of the fouling resistance with time at various flow velocities. The Re varied from 2552 to 5578 by changing the solution flow rate from 0.3 to 0.9 $\text{m}^3 \text{h}^{-1}$ with the fixed CaSO_4 concentration, chevron angle, and inlet temperatures of the solution and hot water. The fouling

resistance decreased and the asymptotic fouling period increased with the increase in the Re because of the increased flow velocity. The deposition rate decreased with the increase in the Re due to more dominant effects of the lower surface temperature, resulting in the lower fouling resistance.

Fig. 6 shows the variation of the pressure drop ratio (ΔP_R) with time at various chevron angles. The CaSO₄ concentration and Re were maintained at 0.6 wt. % and 2512 – 2602, respectively. The inlet temperature of the hot water and solution was fixed at 95 °C and 40 °C, respectively. As the chevron angle increased from 30° to 60°, the increasing rate of the pressure drop ratio increased because the increased fouling deposit led to the decrease in the flow channel diameter. The higher chevron angle resulted in the increased shear stress between the heat transfer surface and laminar flow boundary layer.

Fig. 7 shows the variation of the pressure drop ratio with time at various CaSO₄ concentrations. The Re, chevron angle, and inlet temperature of the solution and hot water were maintained at 2552 – 2601, 60°, 40 °C, and 95 °C, respectively. The increasing slope of the pressure drop ratio increased with the increase in the CaSO₄ concentration because the increased deposition rate led to the decreased channel diameter and the increased flow velocity. In the CaSO₄ concentration of 0.6 wt. %, the increasing slope of the pressure drop ratio was much higher than that of other two cases because the excessively formed deposit with the higher supersaturated condition caused the block of the flow channel at the outlet of the PHE.

Fig. 8 shows the variation of the pressure drop ratio with time at various flow velocities. The Re varied from 2552 to 5578 by changing the solution flow rate from 0.3 to 0.9 m³ h⁻¹ with the fixed CaSO₄ concentration, chevron angle, and inlet temperatures of the solution and hot water. The pressure drop ratio decreased with the increase in the Re because of the increased flow velocity. The increased flow velocity at the interface of the fouling layer and solution also led to higher shear force and smaller residence time of the eddy vortex on the corrugated surface, resulting in the higher pressure drop ratio. On the other hand, the asymptotic period of the pressure drop ratio could be observed at the Re of 3962. The excessive formation of deposit led to the gradual increase in the pressure drop ratio at the lower Re. However, as the Re increased, the decreased deposition rate with the decrease in the surface temperature caused the suppression of the deposit precipitation on the heat transfer surface, resulting in the equilibrium between the deposition rate and removal rate. In the Re of 5578, the pressure drop ratio increased slightly and gradually with time because of the increased flow velocity with the decreased flow channel diameter.

Fig. 9 shows visualization of CaSO₄ crystallization fouling on the heat transfer surface. Based on the visualization tests, severe CaSO₄ crystallization fouling was observed near the gasket because of the stagnant flow near the gasket. The fouling thickness on the surface increased along with the upward flow direction due to the increase in the surface temperature.

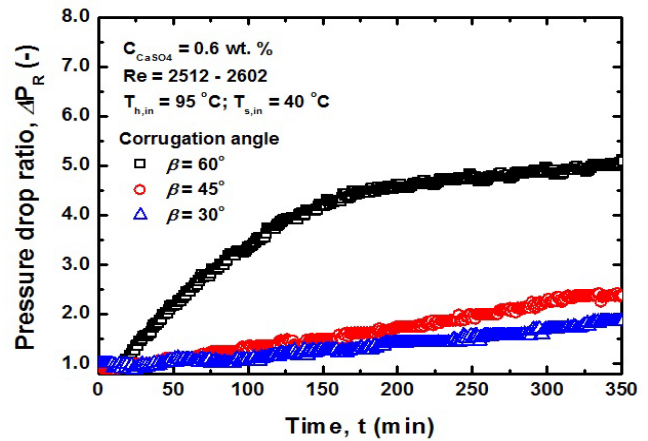


Fig. 6 Effect of chevron angle on the pressure drop ratio.

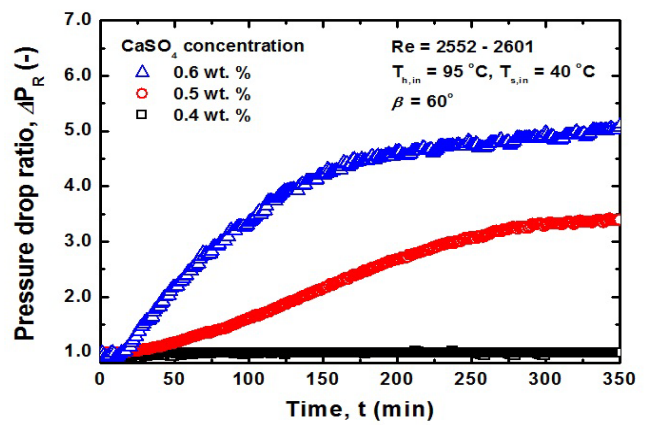


Fig. 7 Effect of CaSO₄ concentration on the pressure drop ratio.

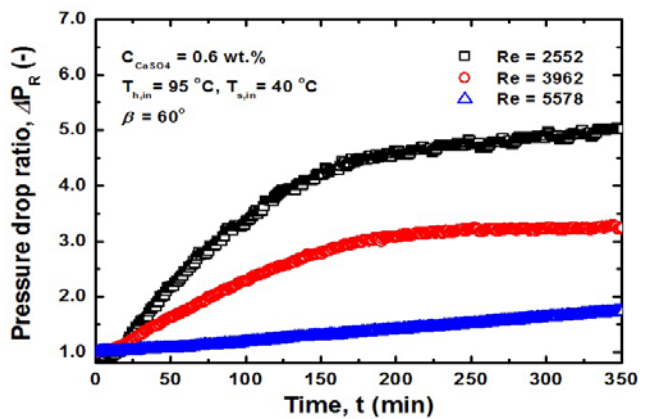


Fig. 8 Effect of Re on the pressure drop ratio.

CONCLUSIONS

In the CaSO₄ crystallization fouling on PHEs, the fouling resistance increased with time and then approached a steady value after a certain period. As the chevron angle increased, the increasing rate of the fouling resistance before the asymptotic fouling period decreased. However, the asymptotic fouling period decreased with the increase in the chevron angle. The asymptotic fouling resistance increased and the asymptotic fouling period decreased with the increase in the CaSO₄ concentration. The fouling resistance decreased and the asymptotic fouling period increased with

the increase in the Re . The increasing rate of the pressure drop ratio (ΔP_R) increased as the chevron angle increased. The increasing slope of the pressure drop ratio increased with the increase in the $CaSO_4$ concentration. The pressure drop ratio decreased with the increase in the Re .



Fig.9 Visualization of $CaSO_4$ crystallization fouling on the heat transfer surface.

Acknowledgements

This work was supported by the Industrial Core Technology Development Program (No. 10049090) of the Korea Evaluation Institute of Industrial Technology (KEIT) funded by the Korea Government Ministry of Trade, Industry and Energy.

NOMENCLATURE

A	heat transfer area, m^2
β	Chevron angle, $^\circ$
C_{CaSO_4}	solution concentration, wt. %)
$C_{p,h}$	hot-side constant pressure specific heat, $kJ\ kg^{-1}\ K^{-1}$
$C_{p,s}$	solution constant pressure specific heat, $kJ\ kg^{-1}\ K^{-1}$
ΔP_R	pressure drop ratio
ΔP_t	pressure drop at a given time, kPa
ΔP_0	pressure drop at clean state, kPa
ΔT_{lm}	logarithmic mean temperature difference, $^\circ C$
m_h	hot-side mass flow rate, $kg\ s^{-1}$
m_s	solution mass flow rate, $kg\ s^{-1}$
Q_{avg}	average heat transfer rate, kW
Q_h	hot-side heat transfer rate, kW
Q_s	solution-side heat transfer rate, kW
Re	Reynolds number
$R_{f,t}$	fouling resistance, $W^{-1}\ m^2\ K$
t	time, min
$T_{h,in}$	hot-side inlet temperature, $^\circ C$
$T_{h,out}$	hot-side outlet temperature, $^\circ C$
$T_{s,in}$	solution inlet temperature, $^\circ C$
$T_{s,out}$	solution outlet temperature, $^\circ C$
U	overall heat transfer coefficient, $kW\ m^{-2}\ K^{-1}$
U_R	thermal performance degradation
U_t	overall heat transfer coefficient at the certain time, $kW\ m^{-2}\ K^{-1}$
U_0	overall heat transfer coefficient at the initial time, $kW\ m^{-2}\ K^{-1}$

REFERENCES

- Bott, T.R., 1997, Aspects of crystallization fouling, *Exp. Therm. Fluid Sci.* 14, 356–360.
- Bansal, B., Müller-Steinhagen, H., Chen, X.D., 2000, Performance of plate heat exchangers during calcium sulphate fouling – investigation with an in-line filter, *Chem. Eng. Proc.* 39, 507–519.
- Bansal, B., Müller-Steinhagen, H., 1993, Crystallization fouling in plate heat exchangers, *J. Heat Transfer* 112, 584–591.
- Dovic, D., Palm, B., Svaic, S., 2000, Visualization of one phase flow in chevron plate heat exchanger and their performance, *J. Mech. Eng.* 46, 429–435.
- Genić, S.B., Jacimović, B.M., Mandić, D., Petrović, D., 2012, Experimental determination of fouling factor on plate heat exchangers in district heating system, *Energy Build.* 50, 204–211.
- Kho, T., Zettler, H.U., Müller-Steinhagen, H., Hughes, D., 1997, Effect of flow distribution on scale formation in plate and frame heat exchangers, *Chem. Eng. Research Des.* 75, 635–640.
- Martin, H., 1996, A Theoretical approach to predict the performance of chevron-type plate heat exchangers, *Chem. Eng. Proc.* 35, 301–310.
- Mayer, M., Bucko, J., Benzinger, W., Dittmeyer, R., Augustin, W., and Scholl, S., 2012, The impact of crystallization fouling on a microscale heat exchanger, *Exp. Therm. Fluid Sci.* 40, 126–131.
- Plummer, L.N., Busenberg, E., 1982, The solubilities of calcite, aragonite and vaterite in CO_2 - H_2O solutions between 0 and 90 $^\circ C$, and an evaluation of the aqueous model for the system $CaCO_3$ - CO_2 - H_2O , *Geochim. Cosmochim. Acta.* 46, 1011–1040.
- Thonon, B., Grandgeorge, S., Jallut, C., 1999, Effects of geometry and flow conditions on particulate fouling in plate heat exchangers, *Heat Transfer Eng.* 20, 12–24.
- Yang, Q., Ding, J., and Shen, Z., 2000, Investigation on fouling behaviors of low-energy surface and fouling fractal characteristics, *Chem. Eng. Sci.* 55, 797–805.